Mon. Not. R. Astron. Soc. **363,** 1167–1172 (2005) doi:10.1111/j.1365-2966.2005.09514.x

Low-order stellar dynamo models

A. L. Wilmot-Smith,[1⋆] P. C. H. Martens,[2] D. Nandy,[2] E. R. Priest[1] and S. M. Tobias[3]

[1]*Mathematical Institute, University of St Andrews, North Haugh, St Andrews KY16 9SS*
[2]*Department of Physics, Montana State University, Bozeman, MT 59717, USA*
[3]*School of Mathematics, University of Leeds, Leeds L52 9JT*

Accepted 2005 August 10. Received 2005 July 29; in original form 2005 June 18

ABSTRACT

Stellar magnetic activity – which has been observed in a diverse set of stars including the Sun – originates via a magnetohydrodynamic dynamo mechanism working in stellar interiors. The full set of magnetohydrodynamic equations governing stellar dynamos is highly complex, and so direct numerical simulation is currently out of reach computationally. An understanding of the bifurcation structure, likely to be found in the partial differential equations governing such dynamos, is vital if we are to understand the activity of solar-like stars and its evolution with varying stellar parameters such as rotation rate. Low-order models are an important aid to this understanding, and can be derived either as approximations of the governing equations themselves or by using bifurcation theory to obtain systems with the desired structure. We use normal-form theory to derive a third-order model with robust behaviour. The model is able to reproduce many of the basic types of behaviour found in observations of solar-type stars. In the appropriate parameter regime, a chaotic modulation of the basic cycle is present, together with varying periods of low activity such as that observed during the solar Maunder minima.

Key words: Sun: activity – Sun: rotation – stars: activity – stars: late-type – stars: rotation.

1 INTRODUCTION

Direct evidence of solar magnetic activity through the observations of sunspots dates back to the early 1600s, with indirect evidence coming from measurements of cosmogenic radioisotopes in tree rings and ice cores over the past 10 000 yr. A systematic record of activity in other late-type stars began in 1966 with the Mt Wilson Ca II H+K project (Duncan et al. 1991; Baliunas et al. 1995; Saar & Brandenburg 1999). This survey has led to many studies on the dependence of activity with such large-scale parameters as stellar age, mass and rotation rate.

The stars in the Mt Wilson survey show several distinct types of activity. Baliunas et al. (1995) divided the stars into four categories based on the variability in their emission: those with no significant variability, those with long-term changes in emission (on a time-scale greater than 20 yr), those with irregular emission, and those with cyclic variation. The Sun itself falls into the final category. The activity periods in the cyclic stars range from around 20 yr to just 2.5 yr, so the Sun's own average cycle period of 11 yr falls in the centre of this range. Considering the sign reversal of the magnetic field along with the 11-yr sunspot cycle gives a periodicity of 22 yr for the solar magnetic cycle. Detailed examination of the sunspot cycle record shows a variation in the length of the activity period from 7 to 17 yr, with a longer-term modulation of the cycle on a period of about 80 yr (the Gleissberg cycle) believed to be present, although not statistically significant. The Sun has undergone several grand minima (Beer, Tobias & Weiss 1998), the last of which being the Maunder minimum during AD 1645–1715 (Eddy 1976; Hoyt & Schatten 1996). Proxy data, for example ^{10}Be in ice cores (Wagner et al. 2001), indicate a statistically significant spectral peak with frequencies corresponding to approximately 205 and 2100 yr (although it is as yet unclear whether this last peak is of solar origin). It is possible that grand minima occur in clusters with a well-defined period of just over 200 yr, and that these clusters reoccur on a time-scale of 2100 yr. There is not currently enough data to allow us to infer similar events in other stars, although some conclusions about stellar magnetic activity can already be drawn.

The Rossby number Ro is a measure of the ratio of the rotation period of a star to its convective turnover time (which is related to the dynamo number D, as $D \propto 1/Ro^2$) and provides an important indicator of rotation rate in these solar-type stars. As stars age, their rotation rate decreases as a result of magnetic braking (Mestel & Spruit 1987), and so their Rossby number increases (implying a corresponding decrease in their dynamo number). It has been shown that the groups of stars with irregular and regular activity are distinguished by their Rossby number (Noyes et al. 1984; Hempelmann, Schmitt & Stępień 1996). Stars with $Ro < 1$ show irregular and strong emission, while the cyclic and constant stars are those with $Ro > 1$. A possible explanation for this division is to explain the magnetic activity as being governed by a non-linear dynamical system whose output changes from constant to periodic to chaotic as a

⋆E-mail: antonia@mcs.st-and.ac.uk

governing parameter (such as the dynamo number) linked to rotation is increased.

From a physical point of view, magnetic activity in solar-type stars is likely to be a result of hydromagnetic dynamo action (Parker 1955; Ossendrijver 2003). Both the components of the stellar magnetic field (i.e. toroidal and poloidal) must be generated by the flow. Thus, any such dynamo model must include a mechanism for the creation of toroidal flux from poloidal flux and also for the regeneration of poloidal flux from toroidal flux. The differential rotation in stellar interiors generates the toroidal field by stretching the poloidal field lines. For the regeneration of the poloidal field from the toroidal component, helical turbulence in stellar convective envelopes, decay of tilted bipolar active regions, various instabilities associated with toroidal magnetic fields and other physically plausible non-axisymmetric mechanisms have been invoked.

Many models of solar and stellar dynamos have been proposed, which qualitatively replicate aspects of the dynamo process, such as flux production, cycle periods and amplitudes, as well as other well-known features observed on the Sun, such as the equatorward drift of sunspots during the cycle and the evolution of the surface radial field; some have included related processes such as magnetic buoyancy and meridional circulation (Ferriz-Mas, Schmitt & Schüssler 1994; Tobias 1996; Nandy & Choudhuri 2002; Brooke, Moss & Phillips 2002; Tobias 2002; Bushby 2003; Ossendrijver 2003; Chan et al. 2004; Charbonneau, Blais-Laurier & St-Jean 2004; Nandy 2004; and references therein). Full simulations of the dynamo process with high magnetic Reynolds numbers that yield strong mean fields are currently out of reach computationally – although see Brun, Miesch & Toomre (2004) for a global simulation of dynamo action in a turbulent rotating spherical shell. Much work has centred on mean-field dynamo theory, with axisymmetric α–ω dynamos attracting the most attention.

A self-consistent magnetohydrodynamic treatment of many of the mechanisms thought to be behind stellar dynamos, such as differential rotation and other large-scale flows, is a formidable task. A different and parallel approach is taken here. We construct a low-order model to examine the bifurcation structure that may be present in the real system. This approach gives one the advantage of exploring a wide variety of stellar behaviour that is governed by the same underlying mathematical structure, without studying each star in detail, or making other modelling assumptions. Thus, this is a complementary study to the works cited in the earlier paragraph.

The construction of low-order models of the solar dynamo has traditionally utilized one of two alternative approaches. The first is to derive sets of ordinary differential equations (ODEs) via a truncation of the partial differential equations (PDEs) of mean-field electrodynamics (Priest 1982; Zeldovich, Ruzmaikin & Sokolov 1983; Martens 1984; Weiss, Cattaneo & Jones 1984; Jones, Weiss & Cattaneo 1985; Schmalz & Stix 1991; Covas & Tavakol 1997; Roald & Thomas 1997). This approach has the advantage that each term in the truncated set of ODEs has an obvious physical interpretation, as it has been derived from an analogous term in the PDEs. However, the drawback of such a procedure is that the dynamics associated with such a truncated model is often fragile and sensitive to the level of truncation. An example of such a truncated dynamo system is given by the Lorenz equations (Knobloch 1981). It is well known that solutions of this set of equations can be steady, periodic or chaotic. In addition, the cycle period decreases with increased driving (rotation). However, the phase relations between the poloidal and toroidal magnetic fields do not match those observed for the Sun.

A second approach is to construct low-order models based on normal-form equations utilizing the theory of non-linear dynamics, by using either symmetry arguments or bifurcation analysis (Tobias, Weiss & Kirk 1995; Knobloch & Landsberg 1996; Knobloch, Tobias & Weiss 1998). Here the dynamics found can be shown to be generic and therefore robust. However, the physical interpretation of the set of low-order equations is less transparent, as there is no obvious physical analogue for a given term in the equations. It is this approach we take here.

The paper is organized as follows. In Section 2 we set-up the model, which is a modification of that first proposed in Tobias et al. (1995). The results of the model are presented in Section 3, followed by conclusions in Section 4.

2 CONSTRUCTION OF THE MODEL

The model considered here is an extension of that derived in Tobias et al. (1995). In that paper, a third-order model was derived using a Poincaré–Birkhoff normal form for a saddle-node–Hopf bifurcation, to obtain a system exhibiting generic and therefore robust behaviour. This normal form was chosen since it has a bifurcation structure that gives qualitatively similar behaviour to that observed in stars as parameters are varied. We expect periodic cyclic solutions to bifurcate from a steady free-field state in a supercritical Hopf bifurcation, in turn giving way to trajectories lying on a two-torus after a secondary Hopf bifurcation. Finally, this cyclic activity should become chaotically modulated to account for those stars with irregular activity. Such a bifurcation structure is mirrored in mean-field PDE models as the non-dimensional measure of rotation rate (the dynamo number D) is increased (Tobias 1996; Pipin 1999; Bushby 2005).

In Tobias et al. (1995) the magnetic field was decomposed in the usual way into its toroidal part, represented by x, and its poloidal part, represented by y. The third coordinate of the system, z, represents all the hydrodynamics, such as differential rotation. The system of ordinary differential equations takes the form

$$\begin{aligned} \dot{z} &= \mu - z^2 - (x^2 + y^2) + cz^3, \\ \dot{x} &= (\lambda + az)x - \omega y + dz(x^2 + y^2), \\ \dot{y} &= (\lambda + az)y + \omega x, \end{aligned} \tag{2.1}$$

where ω and λ give the basic linear cycle frequency and growth rate of x and y, while μ, which is taken to be positive, is the controlling parameter for the hydrodynamics of the system, and so it is related to effects such as thermal forcing and rotation. The parameters a and c have no obvious physical interpretation and have the effect of distorting the bifurcation diagram and removing the degeneracy of the secondary Hopf bifurcation (see Tobias et al. 1995 for details). Of particular importance here is the parameter d, which breaks the axisymmetry, making the system fully three-dimensional, whilst maintaining the invariance of the z-axis.

In order to exhibit the type of behaviour that such a model yields, Tobias et al. (1995) fixed all parameters except for λ and μ. They chose a parametrized path through the λ–μ plane to demonstrate the bifurcation structure that could occur in such a model. In particular, they showed that, as the controlling parameter was increased, purely hydrodynamic solutions lost stability in a primary Hopf bifurcation to oscillatory solutions. In turn these gave way to quasi-periodic solutions, where the basic cycle is modulated on a longer time-scale and solutions lie on a two-torus in phase space. Further increase in the parameter leads to a breakdown of the torus and a transition to chaos. The solution now takes the form of active periods interspersed chaotically with minima. These solutions are associated with close approach to an invariant manifold and near heteroclinicity.

However, as noted by Ashwin, Rucklidge & Sturman (2004), a limitation of the model is that the choice of term to break the normal-form axisymmetry in Tobias et al. (1995) results in a loss of equivalence of the system under the transformation $x \to -x$, $y \to -y$, which corresponds to $B \to -B$. Here we choose an alternative term, which does not suffer from the above disadvantage, to break the axial symmetry. We add a term proportional to $(x^3 - 3xy^2)$ to the x equation and one proportional to $(3x^2y - y^3)$ to the y equation. Thus the model becomes

$$\begin{aligned} \dot{z} &= \mu - z^2 - (x^2 + y^2) + cz^3, \\ \dot{x} &= \lambda x - \omega y + azx + d(x^3 - 3xy^2), \\ \dot{y} &= \lambda y + \omega x + azy + d(3x^2y - y^3). \end{aligned} \tag{2.2}$$

This new system of equations is invariant under the transformation $x \to -x$, $y \to -y$ and the z-axis remains invariant. The physical advantages of our choice become clear when the system is written in cylindrical polars:

$$\begin{aligned} \dot{z} &= \mu - z^2 - r^2 + cz^3, \\ \dot{r} &= (\lambda + az)r + dr^3 \cos(2\phi), \\ \dot{\phi} &= \omega + dr^2 \sin(2\phi). \end{aligned} \tag{2.3}$$

In the following section we examine some of the properties of this model.

3 RESULTS

We examine the behaviour of the system as λ and μ are varied and fix the parameters a, c, d and ω as

$$a = 3, \qquad c = -0.4, \qquad d = 0.4, \qquad \omega = 10.25.$$

Following Tobias et al. (1995) we have chosen to fix $a = 3$ and $c = -0.4$ so that both the line of saddle-node bifurcations at $\mu = 4/27c^2$ and secondary Hopf bifurcations at $\lambda = -2a/3c$ are far from the origin, as shown in Fig. 1. As with system (2.1), the choice of ω does not greatly affect the bifurcation structure, but it does change the ratio of the modulation cycle to the underlying cycle. We have chosen $\omega = 10.25$, since it results in a ratio similar to that observed in the Sun.

To allow us to choose a suitable path through parameter space along which to study solutions of (2.2), we examine the bifurcation set for the system; this is shown in Fig. 1. We see that the line of secondary Hopf bifurcations, which for $d = 0$ was identical to the positive μ-axis, has moved leftward in our new model (2.2). A heteroclinic region, which is shaded in the diagram, replaces the degenerate heteroclinic bifurcation that exists when $d = 0$, as in Tobias et al. (1995). We have not indicated all the bifurcations lying inside this wedge owing to the complexity of the region, some details of which are described in, for example, Champneys & Kirk (2004). The main dynamical features observed are described as follows.

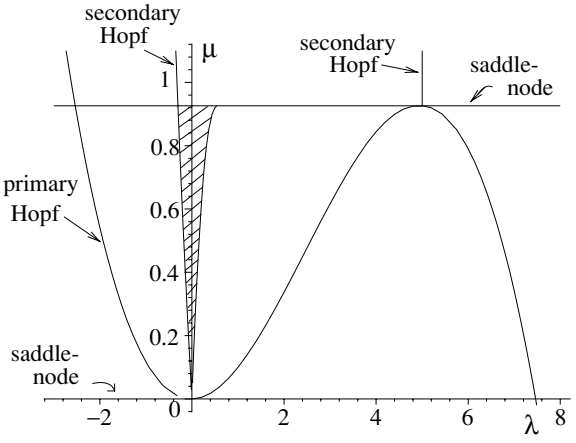

Figure 1. Bifurcation set for equation (2.2) with $a = 3$, $c = -d = 0.4$ and $\omega = 10.25$.

Trajectories within this region lie on a torus, and the rotation number associated with each orbit may be either rational or irrational. In the case of a rational rotation number, p/q ($p, q \in \mathbb{Z}$), since the z-axis is invariant under the flow, the orbit will turn q times around the z-axis and p times around the primary periodic orbit before closing in on itself. This resonance phenomenon does not occur when the rotation number is irrational; in this case no point on the torus is revisited in a finite time. The resonance regions are found to be slim tongues that open out smoothly from the secondary Hopf bifurcation, and are bounded by curves of saddle-node bifurcations of periodic orbits (Kirk 1991). Horseshoes are introduced into the flow, resulting from the heteroclinic crossings of the stable and unstable manifolds of two of the fixed points, and this can lead to chaotic dynamics within the region (Kirk 1991).

To illustrate the new dynamics, we examine the model's behaviour along a one-parameter path in the λ–μ plane, chosen so that solutions along the path mimic the observed stellar behaviour as rotation rate is increased. We choose the parametrization

$$\begin{aligned} \mu &= \sqrt{\Omega}, \\ \lambda &= \tfrac{1}{4}\left\{\left[\ln(\Omega) + \tfrac{1}{3}\right] \exp\left(-\tfrac{1}{100}\Omega\right)\right\}, \end{aligned} \tag{3.1}$$

where $\Omega \in [0, \infty)$, which is similar to that used in Tobias et al. (1995). Clearly the path satisfies the requirement $\mu > 0$. It passes through the primary Hopf bifurcation to the left of the μ-axis and then through the heteroclinic region, staying close to the μ-axis (which is where the complicated dynamics occur). The path then tends back to this axis to give stable dynamo action as $\Omega \to \infty$.

In this section we present the numerical results obtained by integrating the system (2.2) using the Runge–Kutta Fehlberg numerical method in MAPLE. Although we can loosely think of Ω as representing the effects of rotation on the system, we cannot link it directly with any physical parameters such as the Rossby number. As we shall show, the behaviour of the system of equations (2.2) along the parametrized path (3.1) is similar to that found by Tobias et al. (1995).

For small Ω, all trajectories are attracted to one of the fixed points that correspond to purely hydrodynamic states. Magnetic instability sets in at $\Omega = 1.336 \times 10^{-2}$ with a primary (supercritical) Hopf bifurcation, so that periodic trajectories are apparent, a typical example of which is shown in Fig. 2. The radius of the periodic orbit grows as Ω is increased, giving solutions for the magnetic field

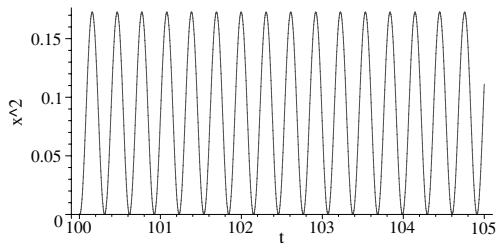

Figure 2. Magnetic activity solution for (2.2) as a function of time along the parametrized path (3.1) at $\Omega = 0.05$. A small-amplitude oscillation is present, whose amplitude grows as Ω is increased.

(represented here by x^2) that grow in amplitude with increasing Ω. The period of oscillation remains approximately constant throughout, since it is controlled largely by the variable ω, with small perturbations to the period arising from the axisymmetry-breaking term.

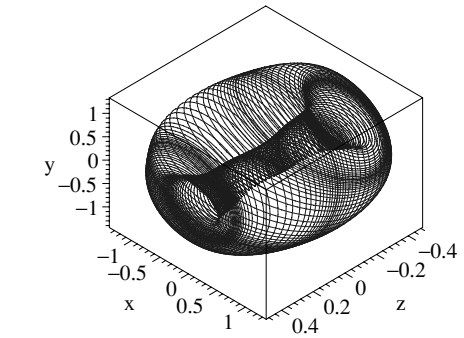

(a)

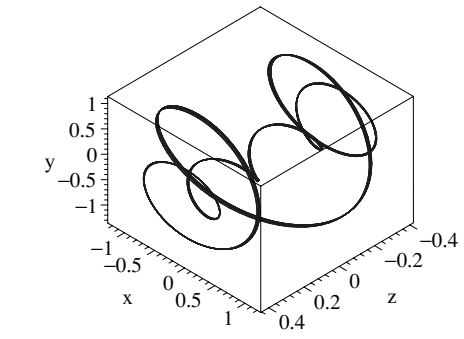

(b)

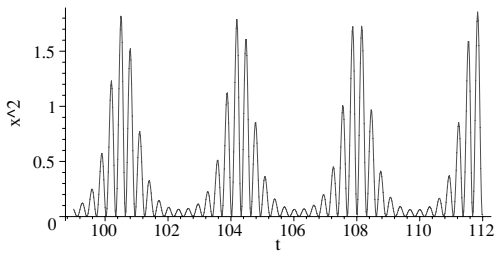

(c)

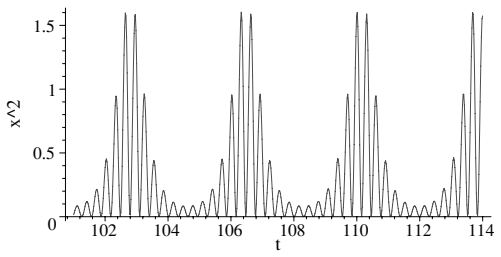

(d)

Figure 3. Solutions to (2.2) along the parametrized path (3.1). The 3D trajectory plot is shown for (a) the quasi-periodic solutions at $\Omega = 0.47$, and (b) the frequency locking at $\Omega = 0.44$. The corresponding activity cycles, represented by x^2, are shown, with (c) $\Omega = 0.47$ and (d) $\Omega = 0.44$.

As the amplitude of the magnetic field grows, the Lorentz force becomes important, varying periodically with half the period of the field, as does the velocity.

At $\Omega = 0.33$ (where $\lambda < 0$), the path crosses the line of the secondary Hopf bifurcation where a torus bifurcates from the periodic orbit. The solutions for $x(t)$ and $y(t)$, which were periodic before the secondary Hopf bifurcation, are now also modulated on a longer time-scale, which results in an oscillatory magnetic field with significant amplitude variations in time. At $\Omega = 0.47$, for example, solutions are quasi-periodic, as shown in Figs 3(a) and (c). Moving along the parametrized path takes us through various

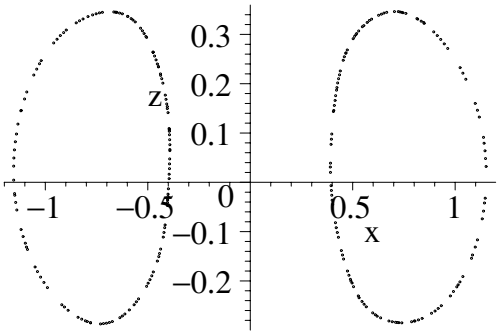

(a)

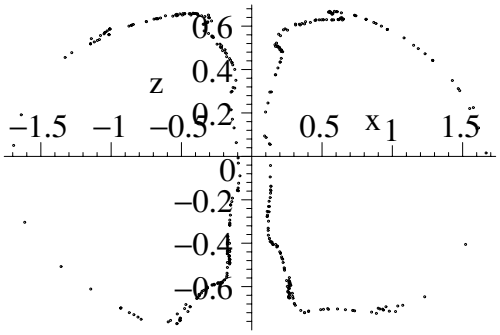

(b)

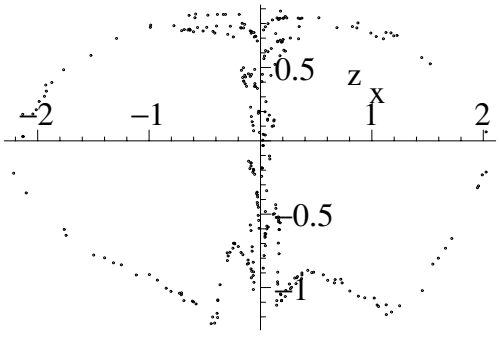

(c)

Figure 4. Poincaré sections through the plane $y = 0$. (a) At $\Omega = 0.35$ the section is well defined and smooth. (b) At slightly larger values of Ω, wrinkles start to appear on the attractor, illustrated here for $\Omega = 0.7$. (c) The transition to chaos is evidenced by folds appearing on the attractor, shown here for $\Omega = 1.3$.

resonance regions, an example of which occurs at $\Omega = 0.44$, as shown in Figs 3(b) and (d). The solutions for $x(t)$ and $y(t)$ appear to be qualitatively similar, but we see that the trajectory winds exactly six times around the z-axis in one period before returning to its original location. Near the frequency-locked regions where the winding numbers are irrational but close to a rational p/q, the orbit can spend most of its time in a phantom periodic orbit from which it occasionally unlocks.

Quasi-periodic solutions do not persist far from the secondary Hopf bifurcation, with the resonance tongues closing off as it is approached. As Ω is increased, the torus grows and begins to approach the invariant z-axis. In addition the torus becomes less smooth, with first wrinkles, then folds developing on the attractor, an effect best illustrated by taking Poincaré sections through the plane $y = 0$. We show this in Fig. 4, where the appearance of folds on the section marks a transition to chaos. The modulation of the underlying cycle in the time series for x and y becomes irregular.

The activity cycle, represented here by x^2, shows irregular bursts of activity followed by variable lengths of no activity. The time series for z (which represents the velocity) oscillates between values near to the two stationary points $z = \pm\sqrt{\mu}$. An example is shown in Fig. 5.

The dynamics is qualitatively unchanged by the saddle-node bifurcation, which is reached at $\Omega = (0.\overline{925})^2 \approx 0.8573$, although two of the three stationary points that existed until this point are destroyed in the bifurcation. The resonance tongues that are associated with the frequency locking of the flow persist (despite the breakdown of the torus), giving rise to windows of periodicity along the trajectory. Close to these regions we again have the situation where the trajectories follow a phantom periodic orbit for much of the time, unlocking only occasionally, an example of which is shown in Fig. 6. In these regions the activity cycle is characterized by sudden and variable increases in the bursts of activity.

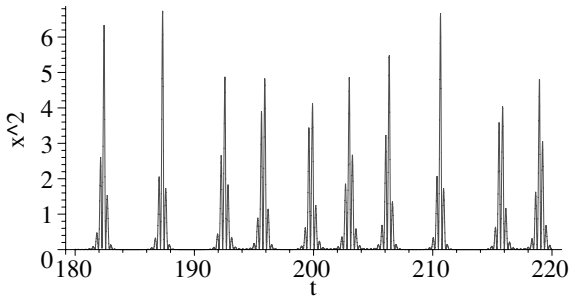

(a)

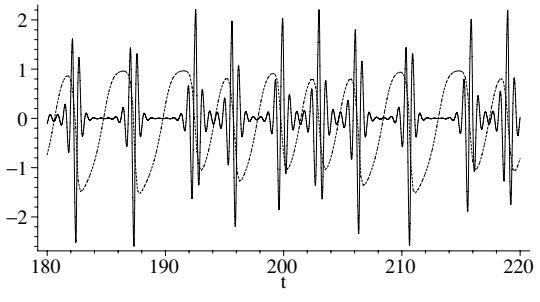

(b)

Figure 5. Chaotic solutions to (2.2) along the parametrized path (3.1) at $\Omega = 1.8$ showing (a) the activity cycle, characterized by bursts of activity between varying periods of very low activity, and (b) $x(t)$ (solid) and $z(t)$ (dotted).

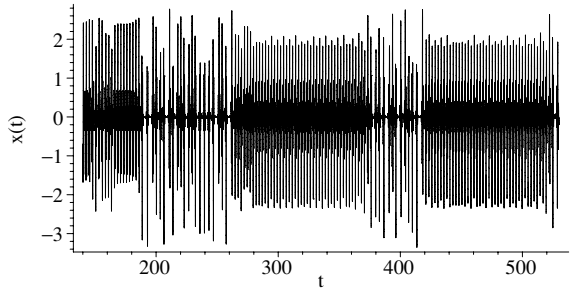

(a)

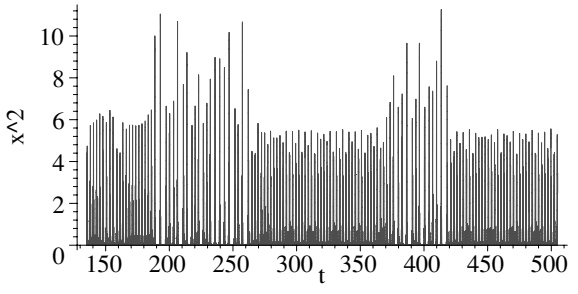

(b)

Figure 6. Solutions to (2.2) along the parametrized path (3.1), close to a frequency-locked region, at $\Omega = 3.35$. The trajectory follows a phantom periodic orbit for much of the time, unlocking occasionally. (a) The solution for the toroidal field $x(t)$ and (b) the activity cycle, which shows occasional sudden increases in activity.

Hence we have shown that the bifurcation structure found for the model of Tobias et al. (1995) remains qualitatively unchanged by the modification of the term that breaks axial symmetry. However, some new interesting dynamics is found in this example. This is illustrated in Fig. 7 for $\lambda = 0.0987$, $\mu = 0.35$, which is not on the parametrized path. It demonstrates that the low-order system is capable of exhibiting clustering of minima, together with periods of reduced and enhanced magnetic activity. We believe that this dynamics is associated with near heteroclinicity and the existence of chaos. The solution occasionally passes very close to the fixed points and the invariant z-axis and this leads to exceptionally deep and long minima. However, for a large proportion of the time, the

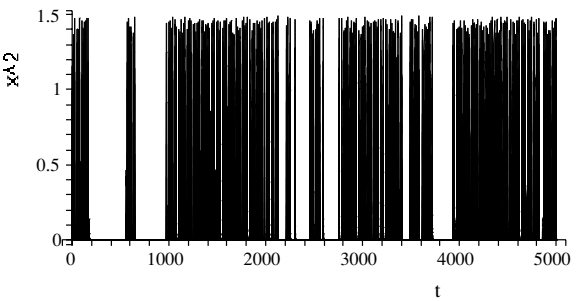

Figure 7. Magnetic activity cycle for $\lambda = 0.0987$, $\mu = 0.35$. Bursts of activity are interspersed with short minima events, with the active periods themselves separated by much longer, deeper minima.

solution is not so close to the invariant manifold and the periods of reduced activity are shorter and clustered with a recognizable period. Extensive searches of the relevant region of parameter space in the model of Tobias et al. (1995) have not located any similar solutions, although we cannot rule out the possibility of their existence.

4 CONCLUSIONS

Our understanding of stellar magnetic activity in solar-like stars and its dependence on parameters such as the Rossby number is deepening through studies such as the H+K project at the Mt Wilson Observatory. The magnetic activity found in this survey divides stars naturally into those with constant emission, periodic emission, irregular emission and long-term changes in emission (Baliunas et al. 1995). Younger stars, which rotate relatively rapidly and have higher dynamo numbers, tend to be those with irregular emission, while older slower rotators (which have low dynamo numbers) tend to show periodic or regular emission (Hempelmann et al. 1996).

Stellar dynamos are governed by highly complex non-linear systems of equations, the modelling of which has been approached in a number of ways, from various types of mean-field model to elaborate numerical simulations. A partial understanding of the bifurcation structure of such models can be gained by studying low-order models, consisting of coupled non-linear ordinary differential equations. Using such a theoretical model one can explore qualitatively the effect of increasing rotation by looking at a system's behaviour in parameter space, for example by increasing the dynamo number. For slow rotators (small dynamo numbers) we would expect to observe a field-free state, with a sequence of bifurcations leading to periodic, quasi-periodic, and finally irregular emission as the dynamo number is increased.

Here we have extended the model of Tobias et al. (1995) to include an axisymmetry-breaking term that maintains the underlying symmetry $B \rightarrow -B$ of stellar dynamos. Many of the parameters can be tied loosely to physical effects; however, since the system has not been derived directly from a set of governing equations, we cannot relate them directly to physical parameters such as the Rossby number. We have demonstrated that the bifurcation sequence proposed by Tobias et al. (1995) is present in the new system of equations, with solutions going from field-free to periodic, quasi-periodic and chaotic as the forcing parameter is increased. Furthermore we have identified a new type of solution that is characterized by the occurrence of long and deep minima interspersed with increased chaotic activity with clusters of shorter minima.

These results are of interest as they can be related to observations, as discussed above. Moreover, the results presented here are robust and so can be related to the bifurcations that are found in more complicated (but less transparent) models based on partial differential equations. Such an analysis of simplified mathematical systems can scientifically complement those numerical studies that attempt either to model fully a particular stellar system or, at a more ambitious level, to solve the full set of magnetohydrodynamic dynamo equations. They can even give a guide as to the types of behaviour to be expected in such systems.

ACKNOWLEDGMENTS

We are very grateful to Nigel Weiss for helpful discussions, and acknowledge the Montana State University Solar Physics Research Experience for Undergraduates program supported by NSF grant ATM-0243923. We acknowledge financial support from the UK Particle Physics and Astronomy Research Council and the NASA TRACE program NAS5-38099. Studies of solar and stellar dynamos at Montana State University are supported by NASA Living With a Star grant NNG05GE47G.

REFERENCES

Ashwin P., Rucklidge A. M., Sturman R., 2004, Physica D, 194, 30
Baliunas S. L. et al., 1995, ApJ, 438, 269
Beer J., Tobias S., Weiss N., 1998, Solar Phys., 181, 237
Brooke J., Moss D., Phillips A., 2002, A&A, 395, 1013
Brun A. S., Miesch M. S., Toomre J., 2004, ApJ, 614, 1073
Bushby P. J., 2003, MNRAS, 342, L15
Bushby P. J., 2005, Astron. Nachr., 326, 218
Champneys A. R., Kirk V., 2004, Physica D, 195, 77
Chan K. H., Liao X., Zhang K., Jones C., 2004, A&A, 423, L37
Charbonneau P., Blais-Laurier G., St-Jean C., 2004, ApJ, 616, L183
Covas E., Tavakol R., 1997, Phys. Rev. E, 55, 6641
Duncan D. K. et al., 1991, ApJS, 76, 383
Eddy J. A., 1976, Sci, 192, 1189
Ferriz-Mas A., Schmitt D., Schüssler M., 1994, A&A, 289, 949
Hempelmann A., Schmitt J. H. M. M., Stępeiń K., 1996, A&A, 305, 284
Hoyt D. V., Schatten K. H., 1996, Solar Phys., 165, 181
Jones C. A., Weiss N. O., Cattaneo F., 1985, Physica D, 14, 161
Kirk V., 1991, Phys. Lett. A, 154, 243
Kirk V., 1993, Physica D, 66, 267
Knobloch E., 1981, Phys. Lett. A, 82, 439
Knobloch E., Landsberg A. S., 1996, MNRAS, 278, 294
Knobloch E., Tobias S. M., Weiss N. O., 1998, MNRAS, 297, 1123
Martens P. C. H., 1984, Phys. Rep., 115, 315
Mestel L., Spruit H. C., 1987, MNRAS, 226, 57
Moss D., Brooke J., 2000, MNRAS, 315, 521
Nandy D., 2004, Solar Phys., 224, 161
Nandy D., Choudhuri A. R., 2002, Sci, 296, 1671
Noyes R. W., Hartmann L. W., Baliunas S. L., Duncan D. K., Vaughan A. H., 1984, ApJ, 279, 763
Ossendrijver M., 2003, A&AR, 11, 287
Parker E. N., 1955, ApJ, 122, 293
Pipin V. V., 1999, A&A, 346, 295
Priest E. R., 1982, Solar Magnetohydrodynamics. Reidel, Dordrecht, p. 338
Roald C. B., Thomas J. H., 1997, MNRAS, 288, 551
Saar S. H., Brandenburg A., 1999, ApJ, 524, 295
Schmalz S., Stix S., 1991, A&A, 245, 654
Tobias S. M., 1996, A&A, 307, L21
Tobias S. M., 2002, Astron. Nachr., 3/4, 417
Tobias S. M., Weiss N. O., Kirk K., 1995, MNRAS, 273, 1150
Wagner G. et al., 2001, Geophys. Res. Lett., 28, 303
Weiss N. O., Cattaneo F., Jones C. A., 1984, Geophys. Astrophys. Fluid Dyn., 30, 305
Zeldovich Ia. B., Ruzmaikin A. A., Sokolov D. D., 1983, Fluid Mech. Astrophys. Geophys., 3, 381

This paper has been typeset from a TEX/LATEX file prepared by the author.